







Optimal Reconfiguration of a Limited Parallel Robot for Forward Singularities Avoidance

Carlos Llopis-Albert¹ , Francisco Valero¹ , Vicente Mata¹ , Rafael J. Escarabajal¹ ,
Pau Zamora-Ortiz¹ , José L. Pulloquina¹ 

¹Centro de investigación de Ingeniería Mecánica (CIIM). Universitat Politècnica de València –
Camino de Vera s/n, 46022 – Valencia, Spain

Corresponding author: Carlos Llopis-Albert, e-mail address: cllopisa@upvnet.upv.es

Received: 18 November 2019; Accepted: 21 March 2020; Published: April 2020

Abstract

The positioning of the anchoring points of a Parallel Kinematic Manipulator has an important impact on its later performance. This paper presents an optimization problem to deal with the reconfiguration of a Parallel Kinematic manipulator with four degrees of freedom and the corresponding algorithms to address such problem, with the subsequent test on an actual robot. The cost function minimizes the forces applied by the actuators along the trajectory and considers singular positions and the feasibility of the active generalized coordinates. Results are compared among different algorithms, including evolutionary, heuristics, multi-strategy and gradient-based optimizers.

Keywords: Parallel robot; non-linear optimization; rehabilitation; trajectory; singularity

1. Introduction

Currently, there is a growing interest in robot trajectory planning (Dash, Chen, Yeo, & Yang, 2005; Rubio, Llopis-Albert, Valero, & Suñer, 2016; Valero, Rubio, & Llopis-Albert, 2019). Different optimization approaches are being proposed for this kind of problems (Llopis-Albert, Rubio, &

Valero, 2018) including the notions, methods, and operations of mobile robots (Rubio, Valero, & Llopis-Albert, 2019).

Particularly, Parallel Kinematic Manipulators (PKMs) has drawn special attention. Compared with serial robots, PKMs can manage higher velocity, accuracy and load capability. However, they exhibit more limited workspace and forward kinematics singularities (Arakelian, Briot, & Glazunov, 2008; Gosselin & Angeles, 1990; Xianwen Kong & Gosselin, 2002), which entail a set of characteristics: a) at least one degree of freedom (DoF) turns uncontrollable; b) they cannot resist some exerted wrenches; c) they are not able to leave such singularity without external help; d) the forces in its joints tend to infinity; and e) it is likely that the manipulator adopts another assembly configuration.

This problem can be tackled by a rigorous trajectory planning of the robot's end-effector, which must consider the avoidance of singularities within the workspace and actuation demands. The reconfiguration of the PKM can help with this task (Patel & George, 2012).

This paper addresses the geometrical redesign of a reconfigurable PKM (RPKM) meant for knee rehabilitation. The trajectories of the mobile platform of the RPKM depend on the patient's rehabilitation procedure and cannot be easily adapted for singularity avoidance (Araujo-Gómez, Díaz-Rodríguez, Mata, & González-Estrada, 2019; Araujo-Gómez, Mata, Díaz-Rodríguez, Valera, & Page, 2017; Vallés et al., 2018). The reconfiguration is treated as a non-linear optimization problem where the design variables are the positions of the four limbs linked to the fixed and mobile platforms, whereas the objective function comprises the total active force needed to follow a defined trajectory subject to several constraints on the value of the determinant of the Forward Jacobian and on the limit values allowed for the active generalized coordinates.

This optimization problem is solved by means of various approaches, including evolutionary algorithms, heuristics optimizers, multi-strategy algorithms and gradient-based optimizers (Yang, 2017). Finally, the results can be compared despite the complexity that the assessment of these optimization algorithms imply (Beiranvand, Hare, & Lucet, 2017).

This paper is organized as follows: Section 2 explains the kinematic and dynamic modeling of the 3UPS+RPU PKM, including the intrinsic forward singularities and the optimization approach.

Section 3 shows the application of the methodology to different cases, and Section 4 states the conclusions.

2. Methodology

2.1. Kinematic model and forward singularities

This paper deals with the optimization of a PKM reconfiguration in order to avoid forward singularities when moving around its workspace. The analyzed PKM is a reconfigurable robot with four DoF (two translations and two rotations) for knee diagnosis and rehabilitation (Vallés et al., 2018). This PKM is named 3UPS-RPU by its architecture, where the underlined letter is the actuated joint. The universal, prismatic, revolute and spherical joints are represented by U, P, R, and S respectively. In Fig. 1 is presented the kinematic modeling implemented for the 3UPS-RPU PKM with 3 identical external limbs and a central limb. In this PKM the actuated joints are the prismatic ones. The fixed reference system is denoted by $\{O_f - X_f Y_f Z_f\}$, while the reference system attached to the mobile platform is given by $\{O_m - X_m Y_m Z_m\}$.

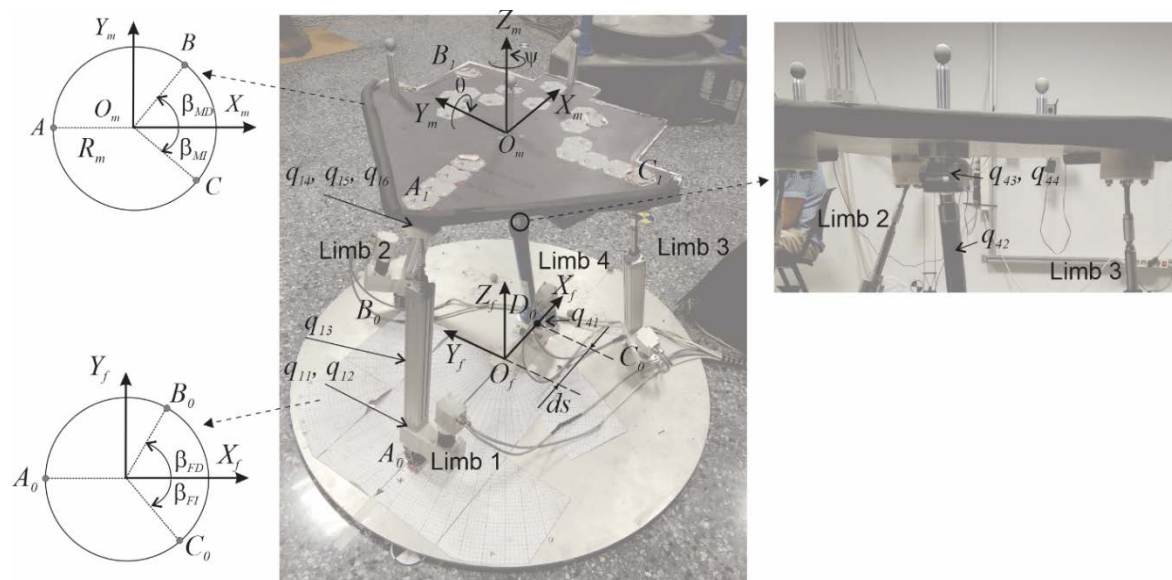


Figure 1. Kinematic modeling for 3UPS-RPU PKM.

The coordinates of the origin of the mobile reference system attached to the mobile platform are x_m and z_m . The angles rotated by the mobile platform regarding Y_m and Z_m are represented by θ and ψ , respectively. Note that y_m and the angle rotated regarding X_m (ϕ) are always zero because of the PKM topology. The location of the connection points to the fixed platform is defined by the radius R , the angles β_{FD} , β_{FI} and the distance ds along the X_f . Regarding the mobile platform, the location of the vertices depend on R_m , β_{MD} and β_{MI} . Eventually, the geometric reconfiguration of the 3UPS-RPU PKM to be minimized is based on 7 geometrical parameters (R , β_{FD} , β_{FI} , R_m , β_{MD} , β_{MI} and ds). This study uses these 7 geometrical parameters as the design variables.

The modeling of the manipulator using Denavit-Hartenberg notation is developed by a set of 22 generalized coordinates q_{ij} (Table 1). The subscript i denotes the number of the limb and j the coordinate within the limb, see Fig. 1.

Table 1. General coordinates in Denavit-Hartenberg notation.

Joint	i	j	α_i	a_i	d_i	θ_i
Universal	1,2,3	1	$-\pi/2$	0	0	q_{ij}
	1,2,3	2	$\pi/2$	0	0	q_{ij}
Prismatic	1,2,3	3	0	0	q_{ij}	0
Spherical	1,2,3	4	$\pi/2$	0	0	q_{ij}
	1,2,3	5	$\pi/2$	0	0	q_{ij}
	1,2,3	6	$\pi/2$	0	0	q_{ij}
Revolute	4	1	$-\pi/2$	0	0	q_{ij}
Prismatic	4	2	$-\pi/2$	0	q_{ij}	π
Universal	4	3	$-\pi/2$	0	0	q_{ij}
	4	4	0	0	0	q_{ij}

The inverse kinematic problem can be posed as a set of explicit expressions in function of the actuated generalized coordinates q_{13} , q_{23} , q_{33} , q_{42} and the design variables:

$$\left. \begin{aligned}
 (q_{13})^2 &= R^2 + (2 \cdot x_m - 2 \cdot C_\theta \cdot C_\psi \cdot R_m) \cdot R + R_m^2 + \\
 &+ (2 \cdot z_m \cdot S_\theta - 2 \cdot C_\theta \cdot C_\psi \cdot x_m) \cdot R_m + x_m^2 + z_m^2 \\
 (q_{23})^2 &= R^2 - 2 \cdot R \cdot \left(\begin{aligned}
 &(C_\theta \cdot C_\psi \cdot C_{FD} \cdot C_{MD} - S_\psi \cdot C_{FD} \cdot S_{MD} + \\
 &+ C_\psi \cdot S_{FD} \cdot S_{MD} + C_\theta \cdot S_\psi \cdot S_{FD} \cdot C_{MD}) \cdot R_m + C_{FD} \cdot x_m \end{aligned} \right) + \\
 &+ R_m^2 - 2 \cdot R_m \cdot (S_\theta \cdot C_{MD} \cdot z_m + S_\psi \cdot S_{MD} \cdot x_m - C_\theta \cdot C_\psi \cdot C_{MD} \cdot x_m) + \\
 &+ x_m^2 + z_m^2 \\
 (q_{33})^2 &= R^2 - 2 \cdot R \cdot \left(\begin{aligned}
 &(C_\theta \cdot C_\psi \cdot C_{FI} \cdot C_{MI} - S_\psi \cdot C_{FI} \cdot S_{MI} + \\
 &+ C_\psi \cdot S_{FI} \cdot S_{MI} + C_\theta \cdot S_\psi \cdot S_{FI} \cdot C_{MI}) \cdot R_m + C_{FI} \cdot x_m \end{aligned} \right) + \\
 &+ R_m^2 - 2 \cdot R_m \cdot (S_\theta \cdot C_{MI} \cdot z_m + S_\psi \cdot S_{MI} \cdot x_m - C_\theta \cdot C_\psi \cdot C_{MI} \cdot x_m) + \\
 &+ x_m^2 + z_m^2 \\
 (q_{42})^2 &= ds^2 - 2 \cdot ds \cdot x_m + x_m^2 + z_m^2
 \end{aligned} \right\} \quad (1)$$

where C_θ , S_θ , C_{FD} , S_{FD} denote $\cos(\theta)$, $\sin(\theta)$, $\cos(\beta_{FD})$, $\sin(\beta_{FD})$, respectively.

The relation between actuated generalized velocities and the velocities of the mobile platform is determinate by time derivate of the equations (1). The velocity relations through a matrix expression is:

$$\Phi_a \cdot \begin{bmatrix} \dot{q}_{13} \\ \dot{q}_{23} \\ \dot{q}_{33} \\ \dot{q}_{42} \end{bmatrix} = \Phi_x \cdot \begin{bmatrix} \dot{x}_m \\ \dot{z}_m \\ \dot{\theta} \\ \dot{\psi} \end{bmatrix} \quad (2)$$

where Φ_a is the Inverse Jacobian and Φ_x the Forward Jacobian.

An inverse singularity is presented when the determinant of Φ_a becomes zero, and a forward singularity occurs with determinant of Φ_x is equal to zero. For the PKM under study, the Φ_a is equal to the identity matrix, which prevent the occurrence of inverse singularities. On the other hand, the Φ_x is a function of the four DoF of the mobile platform (x_m , z_m , θ , ψ). In that case, the 3UPS+RPU PKM will undergo a forward singularity.

2.2. Dynamic model

The dynamic model of the parallel manipulator can be obtained by applying the D'Alembert's Principle and the Principle of Virtual Power (Tsai, 1999):

$$\begin{aligned} -\vec{Q}_{in} + \Phi_q^T \cdot \vec{\lambda} &= \vec{Q}_{grav} + \vec{Q}_{ex} + \vec{Q}_{fric} + \vec{Q}_{act} \\ \Phi_q \cdot \vec{\ddot{q}} &= \vec{b} \end{aligned} \quad (3)$$

Where:

- \vec{Q}_{grav} The gravitational generalized forces
- \vec{Q}_{in} The inertial generalized forces
- \vec{Q}_{fric} The friction generalized forces
- \vec{Q}_{ex} The external generalized forces applied to the mobile platform
- \vec{Q}_{act} The active generalized forces exerted by the actuators
- Φ_q The restriction Jacobian matrix
- $\vec{\lambda}$ The vector of Lagrange multipliers
- $\vec{\ddot{q}}$ The generalized accelerations and
- \vec{b} The vector comprising the acceleration terms quadratic in velocities.

The \vec{q} is a set of generalized coordinates from the active (independent) and passive joints (secondary), organized as:

$$\vec{q} = \left[\begin{array}{c} \underbrace{q_{11}, q_{12}, q_{21}, q_{22}, q_{31}, q_{32}, q_{41}, x_m, z_m, \theta, \psi}_{\text{Secondary } (q^s)} \quad \underbrace{q_{13}, q_{23}, q_{33}, q_{42}}_{\text{Independent } (q^i)} \end{array} \right]^T \quad (4)$$

For the 3UPS+RPU PKM, the Φ_q matrix is defined by deriving respect to \vec{q} the subsequent 11 constraint equations:

$$\begin{bmatrix} C_{11} \cdot S_{12} \cdot q_{13} - R - x_m + R_m \cdot C_\theta \cdot C_\psi \\ -C_{12} \cdot q_{13} + R_m \cdot C_\theta \cdot C_\psi \\ S_{11} \cdot S_{12} \cdot q_{13} - z_m - R_m \cdot S_\theta \\ C_{21} \cdot S_{22} \cdot q_{23} + R \cdot C_{FD} - x_m - R_m \cdot C_{MD} \cdot C_\theta \cdot C_\psi + R_m \cdot S_{MD} \cdot S_\psi \\ -C_{22} \cdot q_{23} + R \cdot S_{FD} - R_m \cdot C_{MD} \cdot C_\theta \cdot S_\psi - R_m \cdot S_{MD} \cdot C_\psi \\ S_{21} \cdot S_{22} \cdot q_{23} - z_m + R_m \cdot C_{MD} \cdot S_\theta \\ C_{31} \cdot S_{32} \cdot q_{33} + R \cdot C_{FI} - x_m - R_m \cdot C_{MI} \cdot C_\theta \cdot C_\psi - R_m \cdot S_{MI} \cdot S_\psi \\ -C_{32} \cdot q_{33} - R \cdot S_{FI} - R_m \cdot C_{MI} \cdot C_\theta \cdot S_\psi + R_m \cdot S_{MI} \cdot C_\psi \\ S_{31} \cdot S_{32} \cdot q_{33} - z_m + R_m \cdot C_{MI} \cdot S_\theta \\ -S_{41} \cdot q_{42} - x_m + ds \\ C_{41} \cdot q_{42} - z_m \end{bmatrix} = \vec{0}_{11 \times 1} \quad (5)$$

Grouping \vec{q} and $\vec{\lambda}$ the Eq. (3) can be rewritten in matrix form, it can be expressed as follows:

$$\begin{bmatrix} M & (\Phi_q)^T \\ \Phi_q & 0 \end{bmatrix} \cdot \begin{bmatrix} \vec{q} \\ \vec{\lambda} \end{bmatrix} = \begin{bmatrix} \vec{Q}_{cc} + \vec{Q}_{grav} + \vec{Q}_{ex} + \vec{Q}_{fric} + \vec{Q}_{act} \\ \vec{b} \end{bmatrix} \quad (6)$$

where \vec{Q}_{in} is divided in the mechanical system mass matrix (M), and the generalized forces related to Coriolis and Centrifugal accelerations (\vec{Q}_{cc}). In this case the 0 is an 11×11 null matrix.

The velocity of the general coordinates (\vec{q}), using coordinate partitioning method (Wehage, Wehage, & Ravani, 2015), can be expressed in function of the independent coordinates as:

$$\vec{q} = \begin{bmatrix} \vec{q}^s \\ \vec{q}^i \end{bmatrix} = \begin{bmatrix} -(\Phi_q^s)^{-1} \cdot \Phi_q^i \\ 1 \end{bmatrix} \cdot \begin{bmatrix} \vec{q}^i \end{bmatrix} = R^* \cdot \begin{bmatrix} \vec{q}^i \end{bmatrix} \quad (7)$$

in this case, Φ_q^i and Φ_q^s are parts of the restriction Jacobian matrix Φ_q related to the independent and secondary generalized coordinates, respectively; 1 is a 4×4 identity matrix.

Multiplying both sides of Eq. (6) by R^* the equation of motion can be compactly written follows:

$$\begin{aligned} (R^*)_{F \times N}^T \cdot (M_{N \times N} \cdot \vec{q}_{N \times 1} - \vec{Q}_{cc_{N \times 1}} - \vec{Q}_{grav_{N \times 1}} - \vec{Q}_{fric_{N \times 1}} - \vec{Q}_{ex_{N \times 1}}) = \\ = (R^*)_{F \times N}^T \cdot \vec{Q}_{act_{N \times 1}} = (R^*)_{F \times N}^T \cdot (Q_{ac_{N \times F}} \cdot \vec{F}_{act_{F \times 1}}) \end{aligned} \quad (8)$$

where N and F are the number of generalized coordinates and the independent coordinates respectively. For this study, $N = 15$ and $F = 4$. $\vec{F}_{act_{F \times 1}}$ are the forces belonging to the actuators on

the PKM. It is worth mentioning that the right-side term $(R^*)_{F \times N}^T \cdot \vec{Q}_{ac_{N \times F}}$ of Eq. (8) is the identity matrix.

The equation of motion can be further developed by considering friction force only in the prismatic actuators, thus only affecting the active generalized coordinates, hence:

$$(R^*)_{F \times N}^T \cdot \left(M_{N \times N} \cdot \vec{q}_{N \times 1} + \vec{Q}_{cc_{N \times 1}} + \vec{Q}_{grav_{N \times 1}} + \vec{Q}_{ent_{N \times 1}} \right) + \vec{F}_{fric_{F \times 1}} = \vec{F}_{act_{F \times 1}} \quad (9)$$

in which the friction force assigned to the generalized active coordinates is represented as:

$$\vec{F}_{fric} = \begin{bmatrix} -\text{sign}(\dot{q}_{13}) \cdot (\mu_c + \mu_v \cdot |\dot{q}_{13}|) \\ -\text{sign}(\dot{q}_{23}) \cdot (\mu_c + \mu_v \cdot |\dot{q}_{23}|) \\ -\text{sign}(\dot{q}_{33}) \cdot (\mu_c + \mu_v \cdot |\dot{q}_{33}|) \\ -\text{sign}(\dot{q}_{42}) \cdot (\mu_c + \mu_v \cdot |\dot{q}_{42}|) \end{bmatrix} \quad (10)$$

where μ_v and μ_c are the viscous and Coulomb coefficients, respectively.

2.3. Objective function and optimization constraints

The reconfigurations process, based on previous works (Araujo-Gómez et al., 2019; Vallés et al., 2018), looks for the optimal set of geometric parameters of the PKM for a specific mobile platform trajectory. The reconfiguration of the 3UPS+RPU (i) prevents Forward singularities inside the workspace (determinant of the Φ_x different from zero), and (ii) avoids large control actions in the vicinity of the singular configurations.

The physical bounds of the seven design variables of the PKM (R , β_{FD} , β_{FI} , R_m , β_{MD} , β_{MI} and ds) showed in Fig. 1 are:

$$\left\{ \begin{array}{l} 0.30 \text{ m} \leq R \leq 0.50 \text{ m} \\ 0.10 \text{ m} \leq R_m \leq 0.30 \text{ m} \\ -0.15 \text{ m} \leq ds \leq 0.15 \text{ m} \\ 0.10 \text{ rad} \leq \beta_{FD} \leq \frac{\pi}{2} \text{ rad} \\ 0.10 \text{ rad} \leq \beta_{FI} \leq \frac{\pi}{2} \text{ rad} \\ 0.10 \text{ rad} \leq \beta_{MD} \leq \frac{\pi}{2} \text{ rad} \\ 0.10 \text{ rad} \leq \beta_{MI} \leq \frac{\pi}{2} \text{ rad} \end{array} \right. \quad (11)$$

The set of rehabilitation trajectories are discretized into a n number of passing through points. At these points we solve the inverse dynamics of the 3UPS+RPU PKM, then we define the objective function as the sum of the square of the active generalized forces (\vec{F}_{act}):

$$f(R, R_m, ds, \beta_{FD}, \beta_{FI}, \beta_{MD}, \beta_{MI}) = \sum_{i=1}^n \sum_{j=1}^4 (F_{ij})^2 \quad (12)$$

To ensure that the $\|\Phi_x\| \neq 0$ for all configurations part of the rehabilitation trajectory, the next constraints must be met:

$$|\|\Phi_x\|_{ref} - \|\Phi_x\|_i| < |\|\Phi_x\|_{ref}|; i = 1, 2, \dots, n \quad (13)$$

with:

$$\|\Phi_x\|_{ref} = \max(\|\Phi_x\|_i); i = 1, 2, \dots, n \quad (14)$$

If both sides of the constraint (13) are squared, it can be rewritten as:

$$2 \cdot \|\Phi_x\|_{ref} \cdot \|\Phi_x\|_i - \|\Phi_x\|_i^2 > 0; i = 1, 2, \dots, n \quad (15)$$

The final optimization constraint is referring to the length of each actuator. The length of the actuated joints must be between the minimum (l_{min}) and maximum (l_{max}) length of each limb.

$$\begin{aligned} l_{min} &\leq q_{i3} \leq l_{max}; i = 1, 2, 3 \\ l_{min} &\leq q_{i2} \leq l_{max}; i = 4 \end{aligned} \quad (16)$$

The minimization of the penalty function (12) subjected to non-linear constraints (15) and (16) represents a non-linear optimization problem. In this study, the optimization problem is solved by several approaches, which covers evolutionary algorithms, heuristics optimizers, multi-strategy algorithms and gradient-based optimizers.

2.4. Optimization approaches comparison

Optimization techniques can be classified as either local (commonly gradient-based) or global (commonly non-gradient based or evolutionary) algorithms. However, it is worth mentioning the difficulties in comparing the performance of several optimization algorithms (Beiranvand et al.,

2017). Therefore, we have carried out the optimization algorithm comparison following the recommendations of those authors.

Our research team used these optimization algorithms:

- a) Evolutionary algorithms (EA), which use mechanisms inspired by biological evolution.
- b) Heuristic methods use a heuristic function to solve the problem.
- c) Multi-strategy algorithms combine the strengths of different approaches.
- d) Gradient-Based are iterative methods using the gradient information.

Using the model FRONTIER framework (www.esteco.com) all these optimization approaches are compared. There is an exhaustive explanation about this optimization algorithm in (Yang, 2017).

3. Case studies

A set of 8 trajectories have been tested for knee rehabilitation. All of them are non-feasible in terms of forward singularities and actuators out of range, so they require a reconfiguration. In Table 2, the characteristics of those trajectories are featured, regarding the motion of the mobile platform as well as the difficulties found during the execution.

Table 2. Test trajectories. (1) Forward singularities, (2) Actuators out of range.

Trajectory	Horizontal	Vertical	Inclined straight line	Ellipse
Constant Orientation	Tr1 (1)	Tr3 (2)	Tr5 (2)	Tr7 (1) and (2)
Variable Orientation	Tr2 (1)	Tr4 (1)	Tr6 (1) and (2)	Tr8 (1) and (2)

The reconfiguration involves 7 design variables, but only 4 are optimized ($R, ds, \beta_{FD}, \beta_{FI}$), while the other 3 are kept constant ($R_m, \beta_{MD}, \beta_{MI}$). The initial parameters of the manipulator are defined in Eq. (17) and are intended to avoid a trivial singular configuration. The physical bounds of the optimized design variables are those presented in Eq. (11). Moreover, the actuator angles must be less than 0.7854 rad and their lengths must lie between 0.575 and 0.775 m.

$$\begin{cases} R = 43 \text{ cm} \\ R_m = 23 \text{ cm} \\ ds = 5 \text{ cm} \\ \beta_{FD} = 45^\circ \\ \beta_{FI} = 48^\circ \\ \beta_{MD} = 90^\circ \\ \beta_{MI} = 100^\circ \end{cases} \quad (17)$$

Table 3 summarizes the results obtained when applying the different optimization strategies for trajectory 2. The optimized design variables avoid forward singularities, which is shown by the fact that the minimum value of Eq. (15) is greater than zero (Table 3). The PiLOPT algorithm presents the best performance. However, results greatly depend on the tuning of the specific parameters of each algorithm, e.g., the stopping conditions, population size or step sizes (Beiranvand et al., 2017). In fact, the main reason why the PiLOPT algorithm outperforms the rest is that it only requires one parameter, which is the number of design evaluations determining when the algorithm stops, occurring when no improvement in the Pareto efficiency is observed.

Table 3. Optimized design variables for trajectory 2.

Algorithm	β_{FD} ($^\circ$)	β_{FI} ($^\circ$)	R (cm)	ds (cm)	Objective Function (N^2)	Minimum value of Eq. (15)
Evolutionary algorithms						
NSGA-II	180	48	40	15	154,547.26	$1.64 \cdot 10^{-4}$
MOGA-II	174	60	42	15	149,220.00	$2.22 \cdot 10^{-4}$
ARMOGA	84	168	32	9	143,290.00	$1.82 \cdot 10^{-4}$
Evolution Strategies	180	48	32	-1	129,375.02	$2.18 \cdot 10^{-4}$
Heuristics optimizers						
MOSA	84	156	32	13	147,530.00	$9.39 \cdot 10^{-5}$
MOPSO	67	21	22	-15	106,449.01	$3.21 \cdot 10^{-4}$
Multi-strategy algorithms						
HYBRID	174	60	42	13	150,060.00	$2.11 \cdot 10^{-4}$
PiLOPT	66	18	22	-15	104,010.00	$1.99 \cdot 10^{-4}$
FAST	177	173	40	15	193,527.55	$1.32 \cdot 10^{-4}$
MEGO	63	21	20	-15	110,761.44	$1.55 \cdot 10^{-4}$
Gradient-based optimizers						
MIPSQP	132	138	30	15	212,920.00	$3.20 \cdot 10^{-5}$

After solving the optimization problem using the PiLOPT algorithm, several results are presented. Fig. 2 shows the geometrical robot reconfiguration from the original robot design for the second trajectory and for both the fixed base (left) and the mobile platform (right).

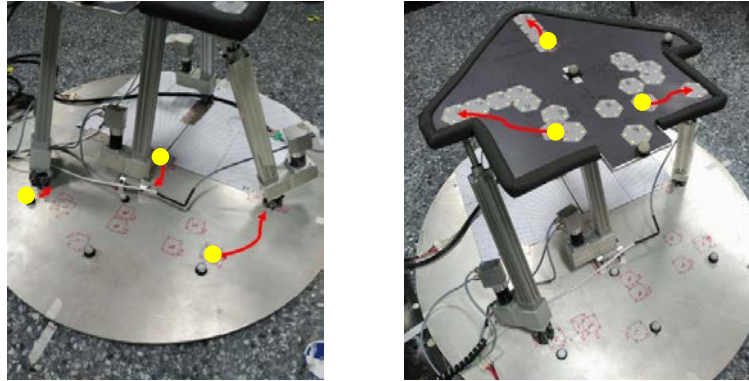


Figure 2. Geometrical robot reconfiguration from the original robot design for the second trajectory and for both the fixed base (left) and the mobile platform (right). The yellow dots correspond to the original configuration of the PKM, while the red lines lead to the final configuration.

Bearing in mind that the PilOPT algorithm leads to the best results, the 8 non-feasible trajectories are solved using this optimization technique. Table 4 illustrates the optimal reconfiguration design variables of the robot using the PilOPT algorithm. The robot reconfiguration prevents high values of generalized forces and the problem of a direct singularity.

Table 4. Optimized design variables for the 8 non-feasible trajectories.

Trajectory	β_{FD} ($^{\circ}$)	β_{FI} ($^{\circ}$)	R (cm)	ds (cm)	Objective Function (N^2)
1	18	30	28	-7	101,130.00
2	66	18	22	-15	104,010.00
3	60	12	30	9	79,627.00
4	60	18	36	15	58,168.00
5	72	30	26	-9	109,410.00
6	48	6	30	1	65,622.00
7	90	25	35	15	83,526.00
8	48	114	32	15	248,780.00

Results show that there is not the best optimization for all types of optimization problems, because each algorithm has its advantages and disadvantages. In general, local algorithms are better when design variables are greater than 50, with high computational cost, with a little significance numerical noise, when local minima are not a problem and when gradients are easily available. Inversely, global algorithms are recommended with less than 50 design variables, with significance

numerical noise, where gradients do not exist, when global optimum is needed and when there are discontinuous objective or constraint functions.

Eventually, global methods should be used only in cases where efficient local search is not feasible.

4. Conclusions

In order to apply the required movements for diagnosis and rehabilitation tasks of anterior cruciate ligament of human knee, a PKM robot with 4 DoF comprised of 3UPS-RPU was designed, and the kinematics and dynamics modeling has been presented. During the execution of certain rehabilitation trajectories, the forward Jacobian becomes singular, so in order to prevent control problems a geometrical and kinematical reconfiguration of the manipulator has been considered. This leads to the achievement of the generalized coordinates that were initially outside range of prismatic actuators.

As it is not possible to modify the rehabilitation trajectories because they are prescribed by the physical therapist, the robot reconfiguration raises as the only solution of such problem. Thus, it is needed to modify the points of insertion of the limbs on both the mobile and fixed robot platforms.

A non-linear optimization solver has been proposed to approach the reconfiguration problem. The penalty function to be minimized sums the square of the active generalized forces. The constraints include the imposition of the robot actuated joints to lie within an admissible range, and the non-singularity of the forward Jacobian.

Using D'Alembert's dynamics inverse model of the PKM and the Principle of Virtual Power the optimal redesign problem of the robot has been tackled. We have used different optimization strategies to solve it. The rehabilitation therapies cover a set of 8 non-feasible trajectories. The second non-feasible trajectory was optimized by using different optimization techniques to find the best one. Results clearly show that the PiLOPT algorithm outperforms the other algorithms for the problem in hand.

The rest of non-feasible trajectories were optimized using PilOPT and the results show that the forces required to carry out these trajectories are much lower than those of the initial configuration of the robot and that the active generalized coordinates fall within the physical ranges of the actuators.

Acknowledgements

This work was supported by the Spanish Ministry of Education, Culture and Sports through the Project for Research and Technological Development with Ref. DPI2017-84201-R.

References

- Arakelian, V., Briot, S., & Glazunov, V. (2008). Increase of singularity-free zones in the workspace of parallel manipulators using mechanisms of variable structure. *Mechanism and Machine Theory*, 43(9), 1129–1140. <https://doi.org/10.1016/J.MECHMACHTHEORY.2007.09.005>
- Araujo-Gómez, P., Díaz-Rodríguez, M., Mata, V., & González-Estrada, O. A. (2019). Kinematic analysis and dimensional optimization of a 2R2T parallel manipulator. *Journal of the Brazilian Society of Mechanical Sciences and Engineering*, 41(10), 425. <https://doi.org/10.1007/s40430-019-1934-1>
- Araujo-Gómez, P., Mata, V., Díaz-Rodríguez, M., Valera, A., & Page, A. (2017). Design and kinematic analysis of a novel 3UPS/RPU parallel kinematic mechanism with 2T2R motion for knee diagnosis and rehabilitation tasks. *Journal of Mechanisms and Robotics*, 9(6), 061004. <https://doi.org/10.1115/1.4037800>
- Beiranvand, V., Hare, W., & Lucet, Y. (2017). Best practices for comparing optimization algorithms. *Optimization and Engineering*, 18(4), 815–848. <https://doi.org/10.1007/s11081-017-9366-1>
- Dash, A. K., Chen, I. M., Yeo, S. H., & Yang, G. (2005). Workspace generation and planning singularity-free path for parallel manipulators. *Mechanism and Machine Theory*, 40(7), 776–805. <https://doi.org/10.1016/j.mechmachtheory.2005.01.001>
- Gosselin, C., & Angeles, J. (1990). Singularity Analysis of Closed-Loop Kinematic Chains. *IEEE Transactions on Robotics and Automation*, 6(3), 281–290. <https://doi.org/10.1109/70.56660>



- Llopis-Albert, C., Rubio, F., & Valero, F. (2018). Optimization approaches for robot trajectory planning. *Multidisciplinary Journal for Education, Social and Technological Sciences*, 5(1), 1. <https://doi.org/10.4995/muse.2018.9867>
- Patel, Y. D., & George, P. M. (2012). Parallel Manipulators Applications—A Survey. *Modern Mechanical Engineering*, 02(03), 57–64. <https://doi.org/10.4236/mme.2012.23008>
- Rubio, F., Llopis-Albert, C., Valero, F., & Suñer, J. L. (2016). Industrial robot efficient trajectory generation without collision through the evolution of the optimal trajectory. *Robotics and Autonomous Systems*, 86, 106–112. <https://doi.org/10.1016/j.robot.2016.09.008>
- Rubio, F., Valero, F., & Llopis-Albert, C. (2019). A review of mobile robots: Concepts, methods, theoretical framework, and applications. *International Journal of Advanced Robotic Systems*, 16(2), 172988141983959. <https://doi.org/10.1177/1729881419839596>
- Tsai, L.-W. (1999). *Robot Analysis and Design*. John Wiley & Sons, Inc. New York, NY, USA ©1999.
- Valero, F., Rubio, F., & Llopis-Albert, C. (2019). Assessment of the Effect of Energy Consumption on Trajectory Improvement for a Car-like Robot. *Robotica*, 37(11), 1998–2009. <https://doi.org/10.1017/S0263574719000407>
- Vallés, M., Araujo-Gómez, P., Mata, V., Valera, A., Díaz-Rodríguez, M., Page, Á., & Farhat, N. M. (2018). Mechatronic design, experimental setup, and control architecture design of a novel 4 DoF parallel manipulator. *Mechanics Based Design of Structures and Machines*, 46(4), 425–439. <https://doi.org/10.1080/15397734.2017.1355249>
- Wehage, K. T., Wehage, R. A., & Ravani, B. (2015). Generalized coordinate partitioning for complex mechanisms based on kinematic substructuring. *Mechanism and Machine Theory*, 92, 464–483. <https://doi.org/10.1016/j.mechmachtheory.2015.06.006>
- www.esteco.com. (n.d.). Retrieved June 10, 2019, from <https://www.esteco.com/>
- Xianwen Kong, B., & Gosselin, C. M. (2002). Kinematics and singularity analysis of a novel type of 3-CRR 3-DOF translational parallel manipulator. *International Journal of Robotics Research*, 21(9), 791–798. <https://doi.org/10.1177/02783649020210090501>
- Yang, X. (2017). *Optimization Algorithms Optimization and Metaheuristic Algorithms in Engineering*. (March). <https://doi.org/10.1007/978-3-642-20859-1>